Journal for ImmunoTherapy of Cancer

Cytoplasmic-delivery of polyinosine-polycytidylic acid inhibits pancreatic cancer progression increasing survival by activating Stat1-CCL2-mediated immunity

Praveen Bhoopathi,[1,2] Amit Kumar,[1,2] Anjan K Pradhan,[1,2] Santanu Maji,[1,2] Padmanabhan Mannangatti,[1,2] Jolene J Windle,[1,2,3] Mark A Subler,[1,2] Dongyu Zhang,[4] Vignesh Vudatha,[4] Jose G Trevino,[3,4] Esha Madan,[3,4] Azeddine Atfi,[2,3,5] Devanand Sarkar,[1,2,3] Rajan Gogna,[1,2,3] Swadesh K Das,[1,2,3] Luni Emdad,[1,2,3] Paul B Fisher [1,2,3]

To cite: Bhoopathi P, Kumar A, Pradhan AK, *et al*. Cytoplasmic-delivery of polyinosine-polycytidylic acid inhibits pancreatic cancer progression increasing survival by activating Stat1-CCL2-mediated immunity. *Journal for ImmunoTherapy of Cancer* 2023;**11**:e007624. doi:10.1136/jitc-2023-007624

► Additional supplemental material is published online only. To view, please visit the journal online (http://dx.doi.org/10.1136/jitc-2023-007624).

Accepted 20 September 2023

For numbered affiliations see end of article.

Correspondence to
Dr Paul B Fisher;
paul.fisher@vcuhealth.org

Dr Luni Emdad;
luni.emdad@vcuhealth.org

ABSTRACT

Background Pancreatic ductal adenocarcinoma (PDAC) is an aggressive cancer without effective therapies and with poor prognosis, causing 7% of all cancer-related fatalities in the USA. Considering the lack of effective therapies for this aggressive cancer, there is an urgent need to define newer and more effective therapeutic strategies. Polyinosine–polycytidylic acid (pIC) is a synthetic double-stranded RNA (dsRNA) which directly activates dendritic cells and natural killer cells inhibiting tumor growth. When pIC is delivered into the cytoplasm using polyethyleneimine (PEI), pIC-PEI, programmed-cell death is induced in PDAC. Transfection of $[pIC]^{PEI}$ into PDAC cells inhibits growth, promotes toxic autophagy and also induces apoptosis in vitro and in vivo in animal models.

Methods The KPC transgenic mouse model that recapitulates PDAC development in patients was used to interrogate the role of an intact immune system in vivo in PDAC in response to $[pIC]^{PEI}$. Antitumor efficacy and survival were monitored endpoints. Comprehensive analysis of the tumor microenvironment (TME) and immune cells, cytokines and chemokines in the spleen, and macrophage polarization were analyzed.

Results Cytosolic delivery of $[pIC]^{PEI}$ induces apoptosis and provokes strong antitumor immunity *in vivo* in immune competent mice with PDAC. The mechanism underlying the immune stimulatory properties of $[pIC]^{PEI}$ involves Stat1 activation resulting in CCL2 and MMP13 stimulation thereby provoking macrophage polarization. $[pIC]^{PEI}$ induces apoptosis via the AKT-XIAP pathway, as well as macrophage differentiation and T-cell activation via the IFNγ-Stat1-CCL2 signaling pathways in PDAC. In transgenic tumor mouse models, $[pIC]^{PEI}$ promotes robust and profound antitumor activity implying that stimulating the immune system contributes to biological activity. The $[pIC]^{PEI}$ anti-PDAC effects are enhanced when used in combination with a standard of care (SOC) treatment, that is, gemcitabine.

Conclusions In summary, $[pIC]^{PEI}$ treatment is non-toxic toward normal pancreatic cells while displaying strong cytotoxic and potent immune activating activities in PDAC, making it an attractive therapeutic when used alone or in conjunction with SOC therapeutic agents, potentially providing a safe and effective treatment protocol with translational potential for the effective therapy of PDAC.

WHAT IS ALREADY KNOWN ON THIS TOPIC

⇒ Pancreatic ductal adenocarcinoma (PDAC) is exceptionally lethal and currently there is no successful method to consistently block or effectively treat PDAC in the clinic, significantly reducing the ability to improve patient outcomes. Polyinosine–polycytidylic acid (pIC), a synthetic double-stranded RNA has been widely used without significant success as an immune adjuvant in many clinical trials for cancer therapy. Delivery of pIC using polyethyleneimine (PEI), facilitates its cytoplasmic entry resulting in cell death in PDAC.

WHAT THIS STUDY ADDS

⇒ We now demonstrate a defining role of the immune system in mediating dramatic survival gains in immune competent transgenic mouse models of PDAC (KPC) when exposed to $[pIC]^{PEI}$, which facilitates entry into the cytosol. Mechanistically, we show for the first time that $[pIC]^{PEI}$ activates Stat1 followed by activation of CCL2 and MMP13 in PDAC, which promotes macrophage polarization. The anti-PDAC actions of $(pIC)^{PEI}$ is enhanced further when combined with gemcitabine, in both human and mouse PDAC cell lines, and KPC mice.

HOW THIS STUDY MIGHT AFFECT RESEARCH, PRACTICE OR POLICY

⇒ This study provides a rationale for the combination of $[pIC]^{PEI}$ with gemcitabine for the therapy of PDAC in patients. Since safety profiles of both $[pIC]^{PEI}$ and gemcitabine are now established, the relevance of our current studies is significant. Our results support the potential for rapid translation of $[pIC]^{PEI}$ into the clinic to treat patients with PDAC to determine efficacy against this invariably fatal cancer.

INTRODUCTION

Pancreatic ductal adenocarcinoma (PDAC) is an aggressive cancer with a dismal prognosis accounting for more than 90% of pancreatic cancers.[1] It is anticipated that in 2030 pancreatic cancer will surpass lung cancer as the second leading cause of cancer-related death in the USA.[2] PDAC responds poorly to systemic treatment, and only 11% of all patients diagnosed with PDAC survive more than 5 years.[3] Current standard of care (SOC) treatments, such as surgery, chemotherapy, and radiation therapy, are only partially effective because of a high level of resistance to these treatments in patients with PDAC.[4] Considering PDAC's aggressive nature and the shortage of existing viable treatments, an imperative exists for developing therapeutic strategies to effectively treat pancreatic cancer.

Identifying oncogenic signaling pathways, understanding resistance mechanisms, targeting genes/pathways involved in PDAC progression and enhancing immune-mediated destruction of PDAC are crucial for developing more effective treatment options.

The immune system is a major contributor to the pathophysiology of pancreatitis and development of PDAC.[5 6] Polyinosinic-polycytidylic acid [pIC], a synthetic analog of double-stranded RNA (dsRNA), interacts with and activates toll-like receptors (TLRs), specifically TLR-3, that are pattern recognition receptors (PRRs) for viruses and dsRNA.[7 8] [pIC] has been used for more than four decades to boost the immune system in an interferon (IFN)-dependent manner.[9] Unfortunately, clinical trials with naked [pIC] documented poor stability and limited IFN induction, as well as no detectable antitumor effects in melanoma and other cancers.[10] Complexing (pIC) with low molecular weight poly-L-lysine, carboxymethylcellulose, liposomes, or polyethylenimine (PEI) increases therapeutic activity via IFN-dependent immune responses.[11–13] The [pIC]LC (Hiltonol), a good manufacturing practice (GMP)-grade stabilized version of [pIC], had improved activity over [pIC],[14 15] and was successfully administered to patients in several clinical trials boosting antitumor immunity.[14 15] These studies suggest that modifying [pIC] may provide enhanced benefit for cancer therapy.

PEI increases transfection efficiency of nucleic acids including DNA, short interfering RNA (siRNA) or RNA in vitro and in vivo.[16] The $[pIC]^{PEI}$ transfers [pIC] into the cytoplasm of tumor cells activating PRRs (TLR-3, RIG-I, or MDA-5) and initiates multiple signaling pathways including NF-κB and IRF3/7 thereby generating effector molecules including proinflammatory factors and type I IFN.[12 17] Treatment of melanoma, breast cancer and hepatoma cells with $[pIC]^{PEI}$ potently suppresses tumor growth and metastasis in animals with an intact immune system.[12 13 18 19] The $[pIC]^{PEI}$ also promotes efficient antitumor activity in mice with defective natural killer, T, or B cell signaling, indicating broad in vivo anticancer activity even in the context of an impaired immune system.[12] Treatment of human PDAC cell lines with $[pIC]^{PEI}$ in vitro or in vivo (nude mice with human tumor xenografts) controls PDAC growth by inhibiting cell proliferation and inducing apoptosis and/or toxic autophagy.[11] Anti-PDAC activity of $[pIC]^{PEI}$ has also been shown in a quasi-orthotopic human pancreatic cancer model where treatment significantly reduced tumor burden in nude mice.[11] Although an involvement of the immune system in determining the anticancer effects of $[pIC]^{PEI}$ in several cancer contexts including PDAC has been proposed,[12 13 17 18] the mechanistic role of the immune system in $[pIC]^{PEI}$ anticancer activity requires further clarification.

To address the role of an intact immune system in vivo in PDAC in response to $[pIC]^{PEI}$ we used the KPC transgenic mouse model that recapitulates PDAC development in patients.[20] In the KPC model, $[pIC]^{PEI}$ had potent anti-PDAC activity significantly extending the survival of tumor bearing mice. Mechanistically, for the first time, we show that $[pIC]^{PEI}$ induces Stat1 activation followed by CCL2 and MMP13 activation in PDAC, serving as a mediator of $[pIC]^{PEI}$-induced macrophage polarization. We demonstrated previously that $[pIC]^{PEI}$ does not induce growth suppression, toxicity or apoptosis/toxic autophagy in normal pancreatic cells.[11] The strong cytotoxic effect and now documented potent immune activating capability of $[pIC]^{PEI}$ in PDAC, without adversely harming normal cells[11] or tissues, makes this molecule a strong candidate to be used alone or in conjunction with other therapeutic agents to create novel, safe, and potentially effective treatments for patients with PDAC.

MATERIALS AND METHODS

Cell lines and reagents

Human PDAC cell lines (PANC-1, Cat No. CRL-1469 and AsPC-1 Cat No. CRL-1682), THP-1 and RAW 264.7 (murine monocyte, macrophage Cat No. SC-6003) cells were purchased from ATCC (ATCC, Manassas, Virginia, USA). ATCC authenticates these cell lines using short tandem repeat analysis. The cell lines were expanded and frozen immediately after receipt. Cultured cells were tested for mycoplasma contamination using a mycoplasma detection kit. mPDX KPC and mPDX KPC-2 cell lines were established from the ascites of two different tumor-bearing KPC (Pdx-1-Cre/K-$ras^{LSL\text{-}G12D}$/$p53^{flox/wt}$) mice as described previously.[21]

Transfections with [pIC] using jetPEI

All treatments were carried out according to the manufacturer's instructions using in vitro jetPEI (Cat No. 101000053, Polyplus, Genesee Scientific, El Cajon, California, USA) transfection reagent. In a 500 mL solution of 150 mmol/L sodium chloride, [pIC] (Cat No. tlrl-pic, InvivoGen, San Diego, California, USA) was combined with jetPEI (1:2) and left for 20 min to allow complex formation before being administered to cells in new media.[11 12]

Plasmid transfections

Plasmid transfection experiments used FuGene HD transfection reagent (Cat. No E2311, Promega, Madison,

Wisconsin, USA) using the manufacturer's protocol. Details provided in online supplemental methods.

Sorting of monocytes using flow cytometry

For sorting, after tumor dissociation, CD45+ cells were positively selected from the tumor lysate by magnetic-assisted cell sorting. Live CD45+CD11b+Ly6G– cells were sorted using a BD FACSAria fusion cell sorter.[22 23] Primary macrophages were derived from bone marrow cells of C57BL/6 mice. Details provided in online supplemental methods.

Western blotting

Western blotting analysis was performed as described.[11] PDAC cells were treated with either $[pIC]^{PEI}$ (0.5 µg/mL) or gemcitabine (Gem) (5 µM) alone or in combination for 48 hours and cells were collected and lysed, or tumors were collected from $[pIC]^{PEI}$-treated animals and single cell suspensions were made and then lysed. Equal amounts of proteins were resolved on sodium dodecyl-sulfate polyacrylamide gel electrophoresis (SDS PAGE), and western blotting analysis was performed as described.[11 21]

Cell proliferation assays

Cell growth was determined using a modified 3-(4,5-dim ethylthiazol-2-yl)−2,5-diphenyltetrazolium bromide assay as described.[11] Details provided in online supplemental methods.

RT-PCR

PDAC cells or RAW 264.7 cells treated with or without $[pIC]^{PEI}$ (0.5 µg/mL) for 48 hours. Total RNA was then extracted, complementary DNA (cDNA) was synthesized, and real-time PCR was performed for different markers as described.[11] Tumors and spleens isolated from $[pIC]^{PEI}$-treated animals were lysed, total RNA was extracted, cDNA was synthesized, and real-time PCR was performed as described.[11]

Terminal deoxynucleotidyl transferase-mediated nick-end labeling assay

Apoptosis induction in tumor sections of mock-treated or $[pIC]^{PEI}$ (1 mg/kg, total eight doses) treated animals was assessed by terminal deoxynucleotidyl transferase-mediated nick-end labeling (TUNEL) (Cat No. 11684795910, TUNEL Kit, Sigma-Aldrich, St. Louis, Missouri, USA) assay as described earlier[11] following the manufacturer's instructions. Details provided in online supplemental methods.

Immunohistochemical analysis

Immunohistochemical (IHC) analysis was done as described previously. Details provided in online supplemental methods.

In vivo studies

Heterozygous p53 KPC mice (Pdx-1-Cre/K-$ras^{LSL\text{-}G12D}$/$p53^{flox/wt}$) and homozygous p53 KPC mice (Pdx-1-Cre/K–$ras^{LSL\text{-}G12D}$/$p53^{flox/flox}$) were bred in the VCU transgenic mouse core facility. All experimental procedures were conducted according to protocols approved by the VCU Institutional Animal Care and Use Committee (IACUC): reference/ID number- AM10183.

Subcutaneous xenograft studies

Non-tumorigenic KPC mice (Pdx-1-Cre negative/K-$ras^{LSL\text{-}G12D}$/$p53^{flox/wt}$) were pretreated with $[pIC]^{PEI}$ (1 mg/kg, intraperitonially (I.P.) injected) and challenged with a total of 1×10^6 mPDX KPC cells to establish subcutaneous tumors on their flanks. In another study, the mPDX KPC cell line was injected subcutaneously into the flank of non-tumorigenic KPC mice. Treatment began when tumors reached approximately 100 mm^3. The $[pIC]^{PEI}$ was given at a dose of 1 mg/kg for both studies and was dissolved in phosphate-buffered saline (PBS), and anti-CCL2 was injected at a dose of 40 µg/mouse for the studies.

Survival study

Heterozygous or homozygous p53 KPC mice were started on a $[pIC]^{PEI}$ treatment regimen (I.P. injections) at 1 month of age. Mice were treated with a combination of Gem (10 mg/kg, Cat No. G6423, Sigma-Aldrich, St. Louis, Missouri, USA) via I.P. injection three times per week. Mice were kept on this treatment until declining health was evident. At that point, mice were sacrificed, and tumors and spleens were collected. Tumor sections were obtained from these mice and subjected to IHC.

Statistical analysis

All data are presented as mean±SD of at least three independent experiments, each performed at least in triplicate. One-way analysis of variance combined with the Tukey post hoc test of means was used for multiple comparisons. Survival mice in the experimental groups were compared using the log-rank test. Statistical differences are presented at probability levels of $p<0.05$.

RESULTS

$[pIC]^{PEI}$ inhibits mouse pancreatic tumor growth

Cytosolic delivery of [pIC] via PEI, $[pIC]^{PEI}$, causes AKT-XIAP-mediated apoptosis in human PDAC both in vitro and in vivo in athymic nude mice.[11] To determine the potential contribution of the immune system to $[pIC]^{PEI}$ mediated anticancer activity we employed genetically engineered mouse models of PDAC, KPC (Pdx-1-Cre/K–$ras^{LSL\text{-}G12D}$/$p53^{flox/wt}$ or $^{flox/flox}$),[21 24] and two independent cell lines established from PDAC KPC tumors generated from this model (mPDX KPC). Treatment of KPC cells with $[pIC]^{PEI}$, inhibited cell proliferation in a dose-dependent and time-dependent manner, reaching ~45% to ~65% growth inhibition at 1 µg/mL after 48 hours as compared with controls (figure 1A). Treatment of human PDAC cells with $[pIC]^{PEI}$ inhibited AKT activation followed by XIAP degradation.[11] Treatment of both mPDX KPC cell lines with $[pIC]^{PEI}$ inhibited phosphorylation of AKT (figure 1B) and promoted XIAP degradation

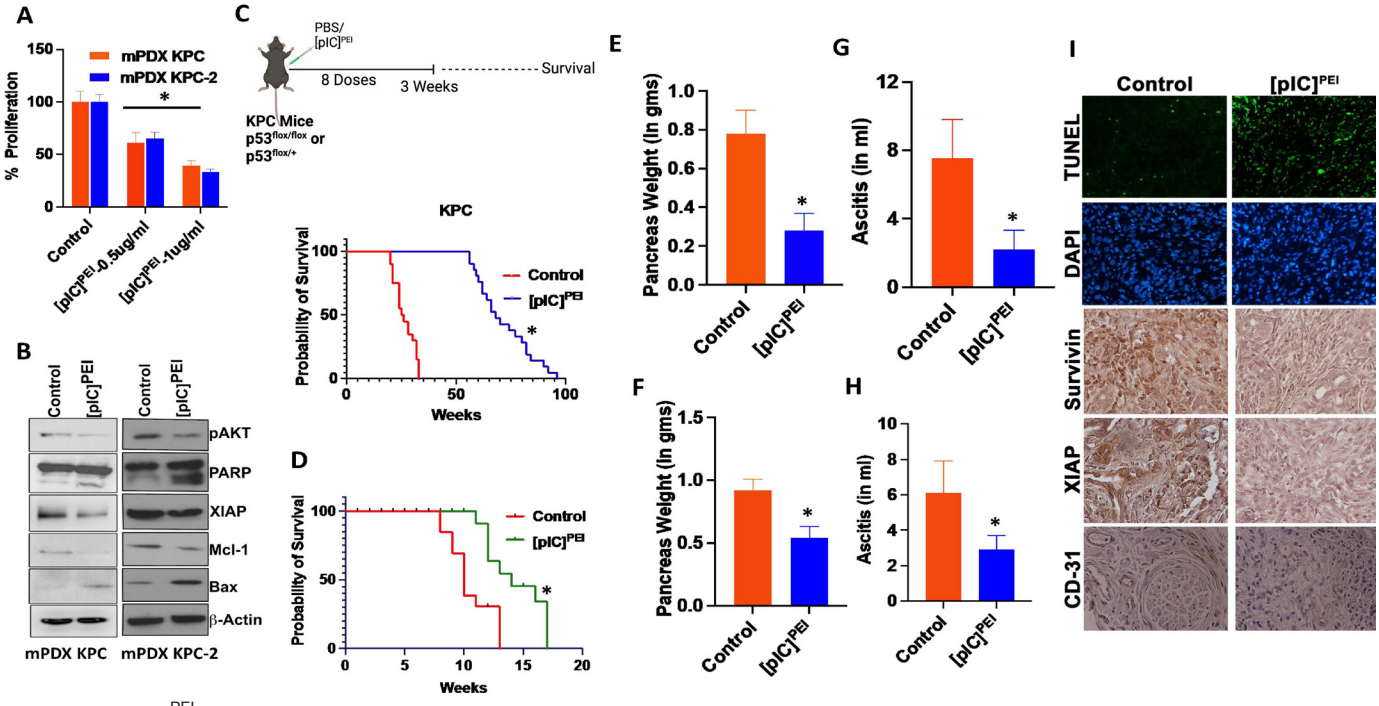

Figure 1 [pIC]^{PEI} inhibits mouse pancreatic tumor growth. (A) Two independently isolated mPDX KPC clones were plated in 96-well plates and treated with the indicated doses of [pIC]^{PEI} for 48 hours followed by MTT assays. Data presented as % proliferation. (B) mPDX KPC cells were treated with [pIC]^{PEI} (1 µg/mL) for 48 hours and western blotting analysis was performed for different marker proteins. (C) Upper panel: Schematic presentation of treatment protocol. Lower panel: Kaplan-Meier survival curve showing significant prolonged survival in heterozygous p53 KPC mice treated with eight doses of [pIC]^{PEI} (1 mg/kg) over 3 weeks. (D) Kaplan-Meier survival curve showing significant prolonged survival in homozygous p53 KPC mice treated with eight doses of [pIC]^{PEI} (1 mg/kg) over 3 weeks. Average pancreas weights (E, F) and average tumor ascites volume (G, H) from KPC mice from C) and D), respectively. (I) TUNEL staining and IHC analysis for Survivin, XIAP and CD31 from control and [pIC]^{PEI}-treated heterozygous mouse tumors. *, p<0.01 compared with control. IHC, immunohistochemistry; MTT, 3-(4,5-dimethylthiazol-2-yl)–2,5-diphenyltetrazolium bromide; PBS, phosphate-buffered saline; PEI, polyethyleneimine; pIC, polyinosine–polycytidylic acid; TUNEL, terminal deoxynucleotidyl transferase-mediated nick-end labeling.

(figure 1B, online supplemental figure S1) as observed in human PDAC cells.[11]

[pIC]^{PEI} has strong antitumor activity in immunodeficient mice when tested using both human PDAC cell line xenografts and in a quasi-orthotopic model, demonstrating that an intact immune system is not mandatory for [pIC]^{PEI} anticancer activity. To determine the effect of [pIC]^{PEI} in immune competent PDAC transgenic mice, KPC mice (heterozygous Pdx-1-Cre/K-ras$^{LSL\text{-}G12D}$/p53$^{flox/wt}$ and homozygous, Pdx-1-Cre/K-ras$^{LSL\text{-}G12D}$/p53$^{flox/flox}$) were either mock treated (PBS) or treated with [pIC]^{PEI} for 3 weeks (eight doses, 1 mg/kg) and survival was monitored. When compared with the mock-treated (PBS) group, mice receiving [pIC]^{PEI} had a dramatic increase in survival in both models. On average, heterozygous KPC mice survived about 6–8 months, whereas [pIC]^{PEI} significantly enhanced mouse survival (>threefold) and some mice were alive >24 months (figure 1C). The [pIC] also enhanced survival (~6–8 weeks), but to a much lower extent than with [pIC]^{PEI} (online supplemental figure S2). In contrast, PEI did not alter survival in heterozygous KPC mice (data not shown). Homozygous KPC mice display shorter survival times (10–14 weeks), however [pIC]^{PEI} extended survival several additional weeks (14–18 weeks) (figure 1D). Tumor mass and ascites volume analyses revealed that [pIC]^{PEI}-treated animals had approximately 50–75% inhibition of tumor growth (figure 1E and F) and a 50–65% reduction in ascites volume (figure 1G and H). To determine if [pIC]^{PEI} also induced AKT-mediated and XIAP-mediated apoptosis in vivo, tumor sections were immunoassayed for Survivin, XIAP and CD31. TUNEL analyses were used to determine apoptotic cells. Tumor sections from [pIC]^{PEI}-treated mice showed decreased expression and H-Score (online supplemental figure S3A) of Survivin, XIAP, CD31 (figure 1I) and pAkt (online supplemental figure S3B), which was consistent with the in vitro findings. Additionally, [pIC]^{PEI} increased the apoptotic index of tumor cells as documented by TUNEL-positive cells. These observations demonstrate that [pIC]^{PEI} retains enhanced anticancer activity in immune competent PDAC animals.

[pIC^{PEI} induces a vaccine effect in KPC mice

We next determined the effect of pretreatment of non-tumorigenic KPC (Pdx-1-Cre negative/K-*ras*$^{LSL\text{-}G12D}$/*p53*$^{flox/wt}$) mice with [pIC]^{PEI} on tumor growth. These mice were treated with [pIC]^{PEI} for 3 weeks (total of eight doses; 1 mg/kg) and challenged with a subcutaneous injection of mPDX KPC cells (1×10^6) (figure 2A). Pretreatment with [pIC]^{PEI} slowed tumor growth as

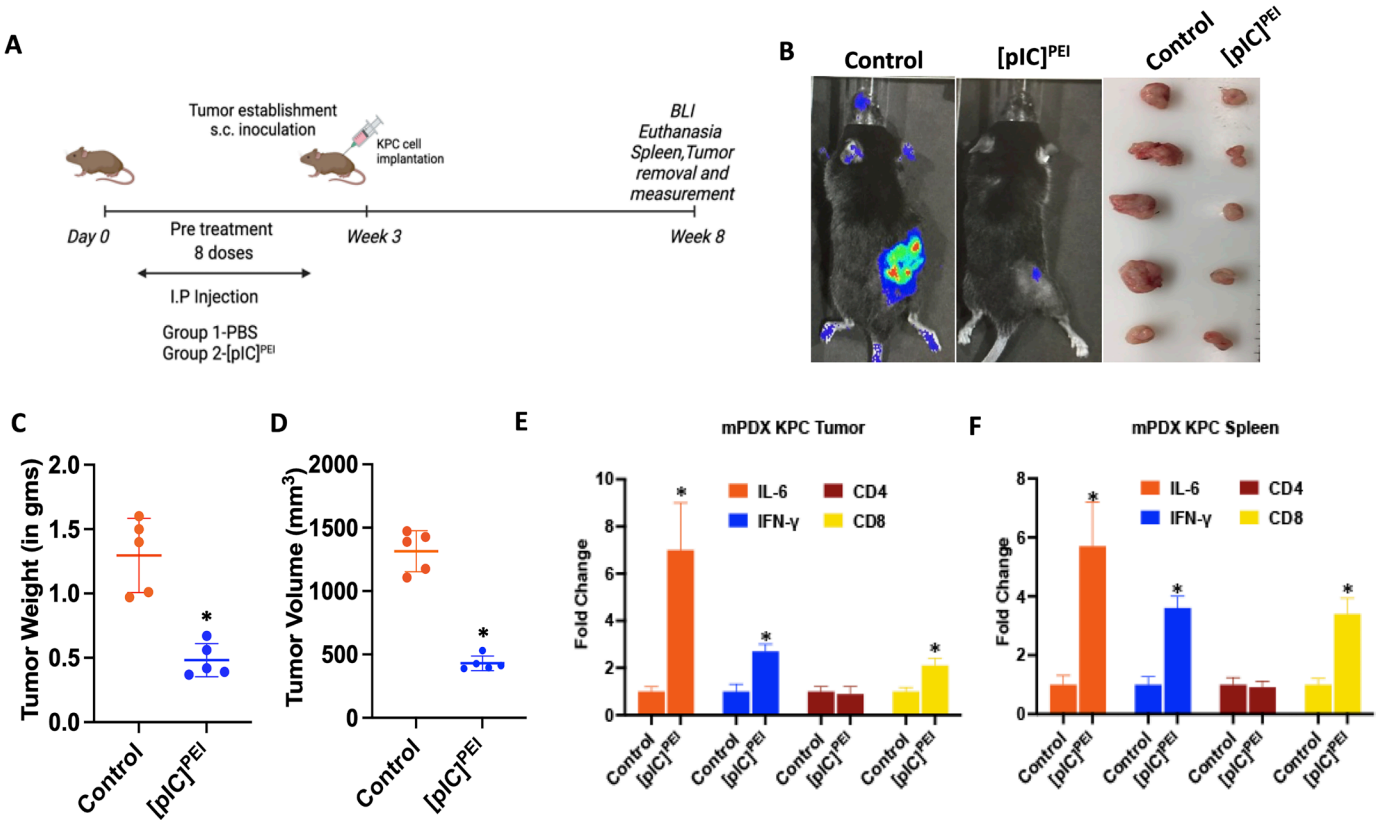

Figure 2 [pIC]^{PEI} potentiates vaccine effect in immune competent mice. Non-tumorigenic KPC mice (Pdx-1-Cre negative/K-*ras*$^{LSL\text{-}G12D}$/*p53*$^{flox/wt}$) were pretreated with eight doses of [pIC]^{PEI} (1 mg/kg) for 3 weeks and challenged with mPDX KPC-Luc cells (1×10^6). (A) Schema of treatment protocol. (B) Left: BLI image in representative animals. Right: Representative photographs of tumors are shown. Average tumor weight (C) and total tumor volume (D) is presented in a graphical manner. (E) Tumors were collected, RNA was isolated, and real-time PCR was performed for IL-6, IFN-γ, CD4 and CD8. (F) Non-tumorigenic KPC (Pdx-1-Cre negative/K-*ras*$^{LSL\text{-}G12D}$/*p53*$^{flox/wt}$) mice were injected intraperitoneally with [pIC]^{PEI} (1 mg/kg). Splenocytes were isolated, processed and real-time PCR was performed for IL-6, IFN-γ, CD4 and CD8. *, p<0.01 compared with control. BLI, bioluminescence imaging; IFN, interferon; IL, interleukin; PBS, phosphate-buffered saline; PEI, polyethyleneimine; pIC, polyinosine–polycytidylic acid; s.c., subcutaneously.

compared with untreated mPDX KPC mice (figure 2B). Control (untreated) mice challenged with subcutaneous implantation of mPDX KPC cells developed large tumors, whereas [pIC]^{PEI}-treated mice challenged with mPDX KPC cells had very small tumors (figure 2B, right panel). Tumor mass and volume analysis revealed that [pIC]^{PEI}-treated animals had an approximately 60% inhibition of tumor growth (figure 2C and D). These results suggest that [pIC]^{PEI} not only promotes tumor cell death, but it also stimulates a 'vaccine effect' in these mice.

Tumors were collected and single cell suspensions were prepared and stained for CD4, CD8 and IFN-γ positive cell populations. CD8+ populations were increased whereas CD4+ populations were unchanged in tumors from [pIC]^{PEI}-treated mice (figure 2E). Additionally, to interrogate systemic activation of immune cells after treatment with [pIC]^{PEI}, non-tumorigenic KPC (Pdx-1-Cre negative/K-*ras*$^{LSL\text{-}G12D}$/*p53*$^{flox/wt}$) mice were injected intraperitoneally with [pIC]^{PEI} (1 mg/kg). Splenocytes were isolated and stained for CD4, CD8, and IFN-γ. [pIC]^{PEI} increased IL-6 in mouse splenocytes (figure 2F). [pIC]^{PEI} also enhanced the levels of CD8+T cells in splenocytes vs untreated mice splenocytes as observed in tumor tissue. CD8+T cells from [pIC]^{PEI}-treated mice produced more IFN-γ (online supplemental figure S4), suggesting systemic activation of tumor/antigen–reactive T cells by local [pIC]^{PEI} therapy.

[pIC]^{PEI} induces Stat1-mediated cell death in KPC cells

IFN-γ is a pluripotent cytokine whose primary biological effects are mediated by the Stat1 transcription factor. IFN-γ also activates Stat3, as part of the IFN response.[25] The [pIC]^{PEI} activates Stat1 and Stat3 via phosphorylation in human and murine PDAC cell lines (figure 3A, online supplemental figure S5A). Elevated levels of pStat1 were evident in KPC mouse tumors treated with [pIC]^{PEI} (online supplemental figure S6). Stat1 signaling in CD8+T cells is essential for effective proliferation by boosting survival of activated CD8+T cells in vivo after virus infection, implying that type I IFNs directly influence CD8+T cells.[26] To examine the role of activated Stat1 in [pIC]^{PEI}-mediated activity in PDAC we developed a Stat1-DN mutant expressing stable mPDX KPC cells (figure 3B, online supplemental figure S5B). Stable

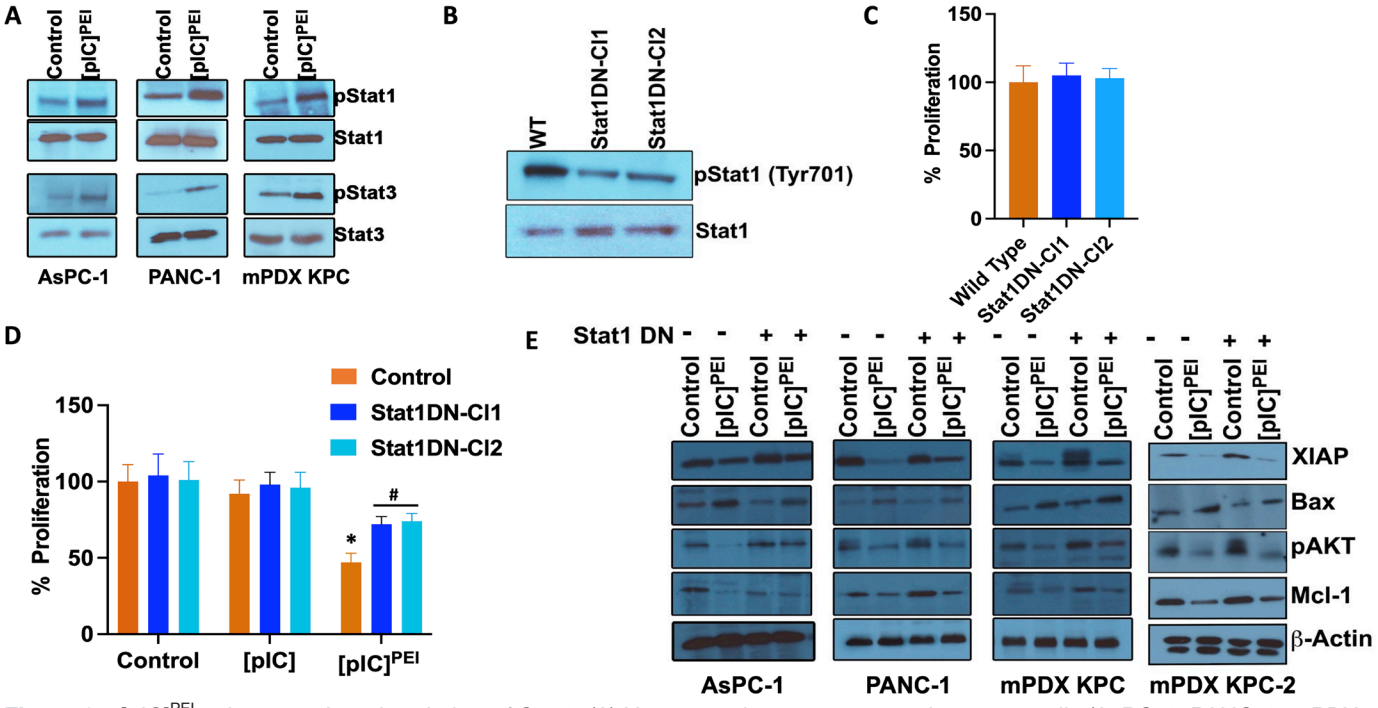

Figure 3 [pIC]^{PEI} enhances phosphorylation of Stat1. (A) Human and mouse pancreatic cancer cells (AsPC-1, PANC-1, mPDX KPC) were treated with [pIC]^{PEI} (0.5 µg/mL) for 48 hours. Western blotting analysis was performed for phopho-Stat1, phospho-Stat3, total Stat1 and Stat3. (B) mPDX KPC cells were transfected with a Stat1-DN plasmid and stable clones were developed. These stable clones were tested for phopho-Stat1 by western blotting analysis. (C) Cell growth was measured using MTT assays in wild type and Stat1-DN mPDX KPC cells 48 hours after plating and percent cell proliferation is shown graphically. (D) Cell growth was measured using MTT assays in wild type and Stat1-DN mPDX KPC cells 48 hours after treatment with [pIC] alone or with [pIC]^{PEI}. Changes in percent cell proliferation are shown graphically. *, p<0.01 compared with control. #, p<0.05 compared with control. (E) human and mPDX KPC pancreatic cancer cells (wild type and Stat1-DN) were treated with [pIC]^{PEI} for 48 hours and western blotting analysis was performed for different pro-apoptotic and anti-apoptotic molecules. β-actin served as loading control. MTT, 3-(4,5-dimethylthiazol-2-yl)–2,5-diphenyltetrazolium bromide; PEI, polyethyleneimine; pIC, polyinosine–polycytidylic acid; WT, wild type.

expression of Stat1-DN in mPDX KPC cells did not affect proliferation (figure 3C). KPC cells stably expressing Stat1-DN were less sensitive to [pIC]^{PEI}-mediated inhibition of cell proliferation (figure 3D). The [pIC]^{PEI} increased expression of Bax and decreased expression of XIAP, pAKT, and Mcl-1, which was reversed by the ectopic expression of the Stat1-DN in human and mouse PDX cells (figure 3E, online supplemental figure S7). In contrast, blocking Stat3 with a Stat3-DN mutant did not promote downstream gene changes (online supplemental figure S8). These results support the importance of Stat1, but not Stat3, activation in [pIC]^{PEI}-mediated PDAC cell death.

[pIC]^{PEI} increases inflammatory cytokine production

Inflammatory monocytes are recognized promoters of cancer,[27 28] and we hypothesized that [pIC]^{PEI} may cause the release of soluble molecules that modify the polarity of inflammatory monocytes in vivo. Treatment of KPC mice with [pIC]^{PEI} increased expression of a plethora of murine cytokines, indicating that [pIC]^{PEI} stimulates the secretion of inflammatory cytokines (figure 4A). Densitometry analysis and heat maps of cytokine arrays revealed that CCL2, CCL5, CXCL10, CXCL13, IL-1Rα and TIMP-1 were elevated in [pIC]^{PEI}-treated KPC mouse serum (figure 4B and C). Messenger RNA (mRNA) levels of these cytokines in tumor samples were also elevated following [pIC]^{PEI} treatment (figure 4D). Treatment of RAW 264.7, murine monocyte/macrophage-like, cells with [pIC]^{PEI} also elevated the mRNA levels of the same cytokines (online supplemental figure S9). The similar profile of enhanced cytokine expression in [pIC]^{PEI}-treated RAW 264.7 cells as observed in the serum of [pIC]^{PEI}-treated KPC mice suggests that macrophages may play a key role in cytokine release in treated PDAC tumors. [pIC]^{PEI} decreased IFN-γ, CCL2 and MMP13 mRNA in tumors established using Stat1-DN KPC cells (figure 4E). Taken together these results indicate that tumor-associated macrophages are likely involved in cytokine expression upon [pIC]^{PEI} treatment. These experiments also show that Stat1 functions downstream of [pIC]^{PEI} as a regulator of CCL2.

[pIC]^{PEI} is involved in M1 macrophage polarization

Macrophages are often polarized into conventionally activated (M1) or alternatively activated (M2) macrophages in response to different therapies.[29] Stat1 enhances M1 macrophage polarization[30] and Stat1 activation/expression is significantly increased in PDAC cells and tissues

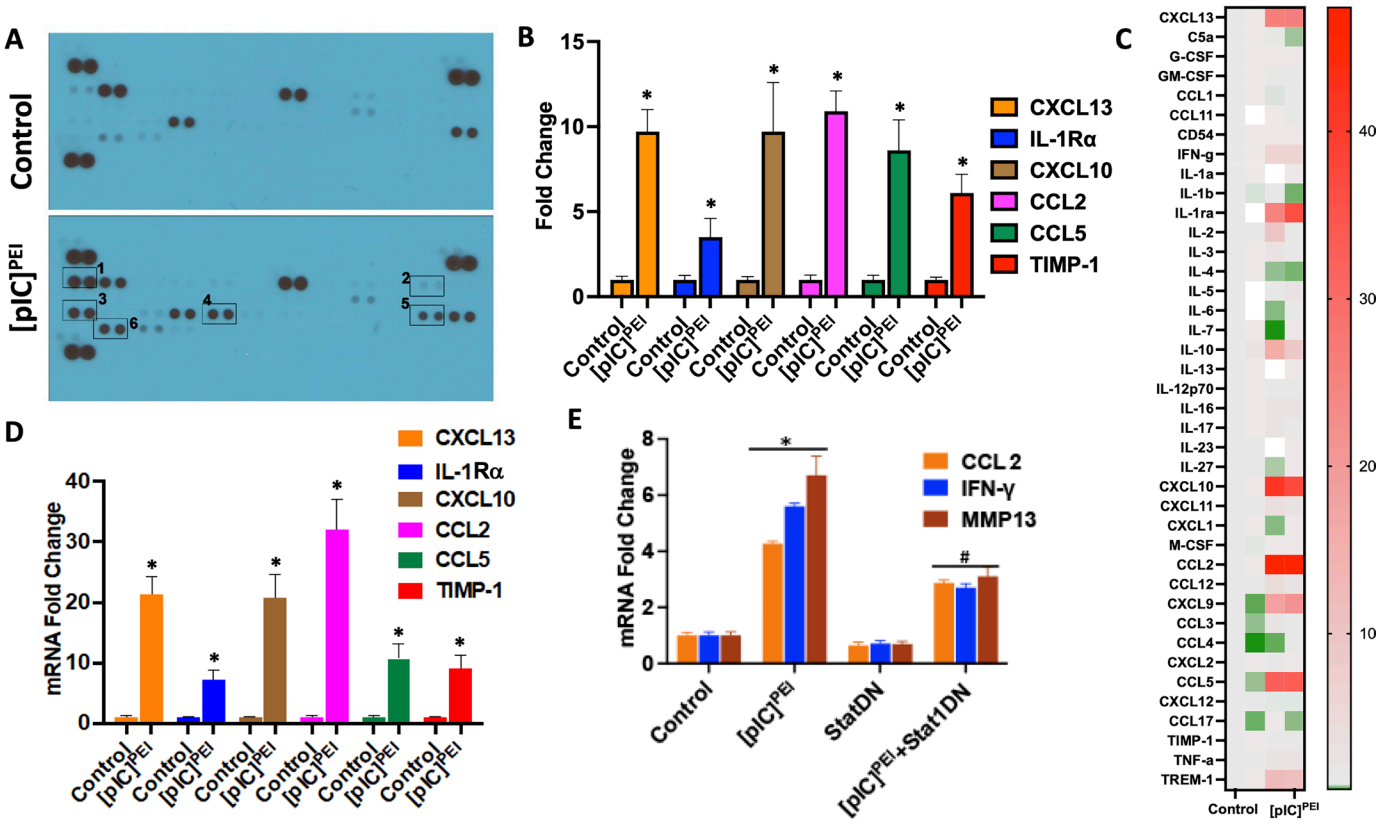

Figure 4 [pIC]^{PEI} treatment alters cytokine profiles in PDAC mice. (A) Homozygous KPC mice were treated with [pIC]^{PEI} for 3 weeks (eight doses; 1 mg/kg) and tumors were collected. Tumor lysates were used to probe mouse cytokine arrays using standard manufacturer's protocol. (B) Densitometry analysis showing changes in cytokine profiles in [pIC]^{PEI}-treated group as compared with control mice. (C) Heat map analysis showing changes in cytokine profiles in [pIC]^{PEI}-treated group as compared with control group. (D) KPC mice were treated with [pIC]^{PEI} as indicated in A, tumors were collected, RNA was isolated, and real-time PCR was performed for the indicated cytokines. (E) KPC wild type mice were challenged with either mPDX KPC parental or Stat1DN cells, and once tumors were palpable, they were treated with [pIC]^{PEI} as described in A. Tumors were collected at the end of the treatment, processed, and real-time PCR was performed for IFN-γ, CCL2 and MMP13. *, p<0.01 compared with control. #, p<0.01 compared with [pIC]^{PEI}. mRNA, messenger RNA; PDAC, pancreatic ductal adenocarcinoma; PEI, polyethyleneimine; pIC, polyinosine–polycytidylic acid.

(figure 3, online supplemental figure S5,S6) following [pIC]^{PEI} treatment. Treating tumors with [pIC]^{PEI} increases LY6C and MHC-II positive cells vs untreated tumors (figure 5A). To confirm which macrophage population increases in tumors, we evaluated the tumors for M1-specific and M2-specific macrophage markers such as NOS2, NLRP3 and RETNLA.[31] The [pIC]^{PEI} treatment increased M1 macrophage markers, whereas it decreased M2 macrophage markers (figure 5B,C). Similarly, in RAW 264.7 cells [pIC]^{PEI} treatment resulted in a dose-dependent increase in M1 macrophage markers, whereas M2 markers were downregulated (figure 5D). We observed similar changes in human monocyte cells (THP-1) when treated with [pIC]^{PEI} (online supplemental figure S10). The role of [pIC]^{PEI} on macrophage differentiation in vivo was further confirmed in splenocytes extracted from KPC mice. There was an increase in M1 markers and a decrease in M2 markers in [pIC]^{PEI}-treated KPC mice when compared with untreated mouse splenocytes (figure 5E).

Dense fibrosis and robust macrophage infiltration are key therapeutic barriers in PDAC therapy.[22] We hypothesized that IFN-γ and CCL2 released systemically in response to [pIC]^{PEI} treatment may cooperate to redirect a subset of Ly6C+CCR2+ monocytes/macrophages to infiltrate tumors and deplete fibrosis. CCL2 is required for Ly6C+ monocyte/macrophage infiltration, whereas IFN-γ is necessary for tumor-infiltrating monocytes/macrophages to shift the profile of matrix metalloproteinases (MMP) in tumors, leading to MMP-dependent fibrosis degradation.[32] To further test the relevance of CCL2 on macrophage polarization by [pIC]^{PEI}, we implanted mPDX KPC cells subcutaneously in wild type mice and once palpable tumors developed treated them with either [pIC]^{PEI} (1 mg/kg), Anti-CCL2 (40 µg/mouse) or both for eight injections over a 3 weeks period. On euthanization single-cell suspensions were made from tumors and FACS analysis was performed for macrophage markers. The [pIC]^{PEI}-induced M1 macrophage populations were depleted in mice that received anti-CCL2 antibody treatment, however, there was no significant change in the M2 macrophage population (figure 5F). These results suggest that anti-CCL2 antibody reverses macrophage markers

Figure 5

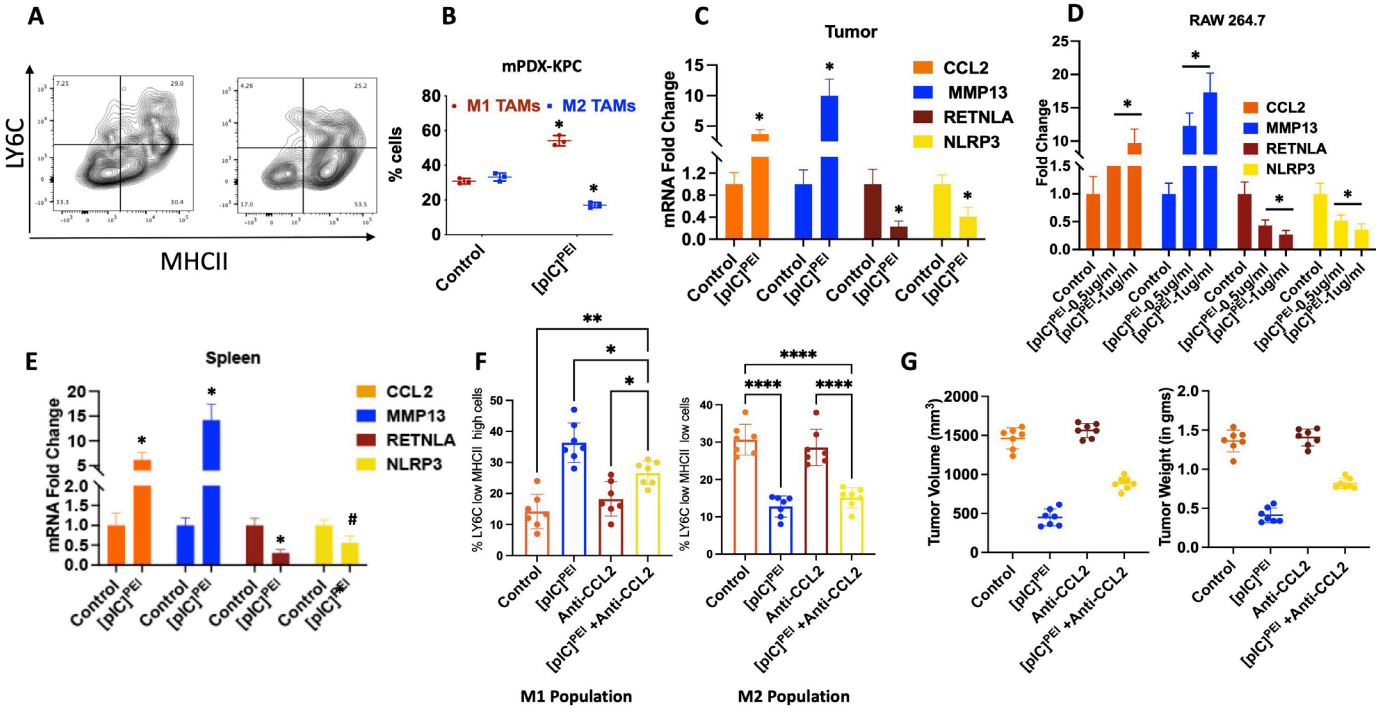

Figure 5 [pIC]^{PEI} facilitates macrophage differentiation. (A) Homozygous KPC mice were treated with [pIC]^{PEI} for 3 weeks (eight doses; 1 mg/kg) and tumors were collected. Single cell suspensions were made from these tumors and stained for macrophage markers. Flow cytometry analysis showing increased macrophage differentiation in [pIC]^{PEI}-treated tumors. (B) Homozygous KPC mice were treated with [pIC]^{PEI} as indicated in A. Tumors were collected, single cell suspensions were made, stained with M1 or M2 specific markers and presented graphically. (C) Homozygous KPC mice were treated with [pIC]^{PEI} as described in A, tumors were collected, RNA was isolated, and real-time PCR was performed for macrophage markers. (D) RAW 264.7 cells were treated with [pIC]^{PEI} (0.5 µg/mL) for 48 hours. These cells were processed, and real-time PCR was performed for macrophage markers. (E) Homozygous KPC mice were treated with [pIC]^{PEI} as described in A. Spleens were processed, and real-time PCR was performed for macrophage markers. *, p<0.01 compared with control; #, p<0.05 compared with control. (F) Homozygous KPC mice were treated with [pIC]^{PEI} as described in A), and/or anti-CCL2 (40 µg/mouse) for three doses in week 3. Tumors were collected, and single cell suspensions were made. Flow cytometry analysis was performed to show the M1 and M2 populations in these individual tumors. (G) Wild type mice were challenged with subcutaneous injections of mPDX KPC cells. Once tumors were palpable, these mice were treated as described in F. Tumor weights and volumes were measured and presented graphically. *, p<0.05 compared with (pIC)^{PEI}+anti-CCL2 **, p<0.01 compared with control, ****, p<0.001 compared with control, anti-CCL2. mRNA, messenger RNA; PEI, polyethyleneimine; pIC, polyinosine–polycytidylic acid.

(M1 populations) in [pIC]^{PEI}-treated tumors, which confirms a role of CCL2 in regulating macrophage polarization in response to [pIC]^{PEI}. Anti-CCL2 also inhibited [pIC]^{PEI}-mediated tumor regression in the mPDX subcutaneous model (figure 5G). Taken together these results suggest that [pIC]^{PEI} helps promote macrophage polarization, which is partly mediated and regulated by CCL2.

[pIC]^{PEI}-mediated macrophage polarization is CCL2-MMP13-dependent in PDAC tumors

Treatment of macrophages with [pIC]^{PEI} in vitro robustly increases MMP13 expression (online supplemental figure S11A), which also occurs in mPDX KPC tumors following [pIC]^{PEI} therapy (online supplemental figure S11B). CCL2 neutralization decreased MMP13 expression in macrophages in vitro and tumors in vivo, confirming the relevance of CCL2 in altering the MMP13 profile in PDAC (online supplemental figure S11C, S12). To determine the effect of an MMP13 inhibitor (MMP13-I) and anti-CCL2 antibody on macrophage polarization, RAW 264.7 cells were treated either with MMP13-I (2.5 µM) or anti-CCL2 antibody (2 µg/mL) for 24-hours and then treated with [pIC]^{PEI} for an additional 36-hours. Inhibition of MMP13 or CCL2 did not alter IFN-γ mRNA levels (online supplemental figure S11E), whereas M1 polarization markers declined (figure 6A,B) suggesting that CCL2 and MMP13 operate downstream of IFN-γ in [pIC]^{PEI}-promoted macrophage polarization. Moreover, MMP13-I did not alter CCL2 or Stat1 in these cells (online supplemental figure S11D, figure 6C, online supplemental figure S13A). Further confirmation of the effect of MMP13-I and anti-CCL2 antibody in macrophage polarization was obtained using bone marrow-derived macrophage (BMDM) cells. BMDM cells were treated similarly as RAW 264.7 cells described above and as was seen in RAW 264.7 cells, inhibition of MMP13 or CCL2 in BMDM cells also inhibited [pIC]^{PEI}-mediated M1 polarization (figure 6D,E). Similarly, inhibition of CCL2 did not alter Stat1 in BMDM (figure 6F, online supplemental figure

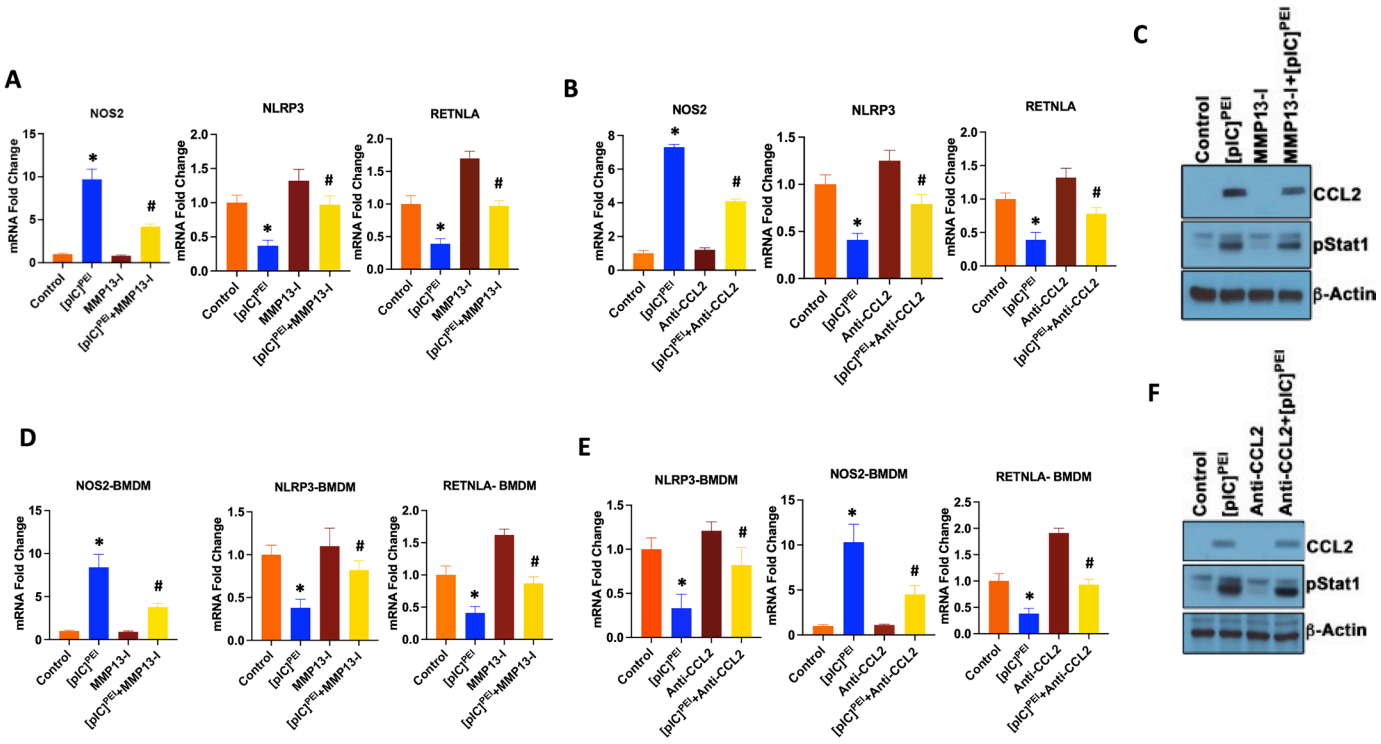

Figure 6 [pIC]^{PEI} induces macrophage differentiation via MMP13 and CCL2. (A) RAW 264.7 cells were treated with [pIC]^{PEI} (0.5 µg/mL) for 24 hours and then challenged with an MMP13 inhibitor (MMP13-I) (2.5 µM) for an additional 24 hours. These cells were collected, RNA was isolated, and real-time PCR was performed for macrophage markers. (B) RAW 264.7 cells were treated with [pIC]^{PEI} (0.5 µg/mL) for 24 hours and then challenged with anti-CCL2 (2 µg/mL) for an additional 24 hours. These cells were collected, RNA was isolated, and real-time PCR was performed for macrophage markers. (C) Bone marrow derived macrophages (BMDMs) were treated as described in A. These cells were collected, and western blotting analysis was performed for CCL2 and p-Stat1. β-actin served as loading control. (D) BMDMs were treated as described in A. These cells were collected, RNA was processed, and real-time PCR was performed for macrophage markers. (E) BMDMs were treated as described in B. These cells were collected, RNA was processed, and real-time PCR was performed for macrophage markers. (F) BMDMs were treated as described in B. These cells were collected, and western blotting analysis was performed for CCL2 and p-Stat1. β-actin served as the loading control. *, p<0.01 compared with control, #, p<0.01 compared with [pIC]^{PEI}. MMP, matrix metalloproteinases; mRNA, messenger RNA; PEI, polyethyleneimine; pIC, polyinosine–polycytidylic acid.

S13B). Taken together these results suggest that [pIC]^{PEI} induces immune-mediated cell death in KPC mice and mPDX KPC cells via the Stat1 pathway, in which CCL2 affects MMP13 in turn regulating macrophage-mediated CD8+T cell activation resulting in immune-mediated cell death. These results demonstrate that [pIC]^{PEI} treatment in KPC mice inhibits PDAC tumor growth by inducing apoptosis in cancer cells and by regulating macrophage polarization via the IFN-γ/Stat1/CCL2 pathway.

[pIC]^{PEI} synergizes with gemcitabine (Gem) in enhancing anticancer activity in PDAC

Despite the fact that PDAC are more responsive to Gem than other anticancer drugs, most patients acquire resistance within weeks of starting treatment, resulting in poor prognosis.[4 33 34] In PDAC, the Akt/mTOR pathway is involved in mediating Annexin II-induced Gem-resistance.[35] This suggests that combining Gem therapy with an mTOR inhibitor may be effective in overcoming Gem-resistance. Based on these considerations, we predicted that combining Gem with an indirect Akt/mTOR inhibitor such as [pIC]^{PEI}, which suppresses the Akt/mTOR pathway,[11] would ameliorate Gem-resistance in PDAC. KPC mPDX cell lines were treated with [pIC]^{PEI} or Gem alone or in combination to investigate the efficacy of chemo-sensitization by [pIC]^{PEI} in inhibiting PDAC proliferation. Significant additive effects were observed between [pIC]^{PEI} and Gem in both inhibiting PDAC proliferation (figure 7A) and triggering apoptosis (figure 7B). Increased Bax and decreased Bcl-2 and pAKT expression was seen in PDAC cells treated with either [pIC]^{PEI} or Gem, which was further augmented following combination treatment (figure 7C, online supplemental figure S14). Additionally, in the homozygous p53 KPC model, an exceptionally aggressive mouse PDAC model in which even a 1-week survival increase is significant, the combination treatment of [pIC]^{PEI} and Gem suppressed PDAC growth and enhanced survival (figure 7D). These effects correlated with a reduced tumor mass and ascites volume in KPC mice when [pIC]^{PEI} was combined with Gem (figure 7E,F). Combination treatment did not result in a further activation/phosphorylation of Stat1 suggesting that additional pathway(s) may contribute to enhanced therapeutic activity of this combination (figure 7G, online supplemental figure S15). Further

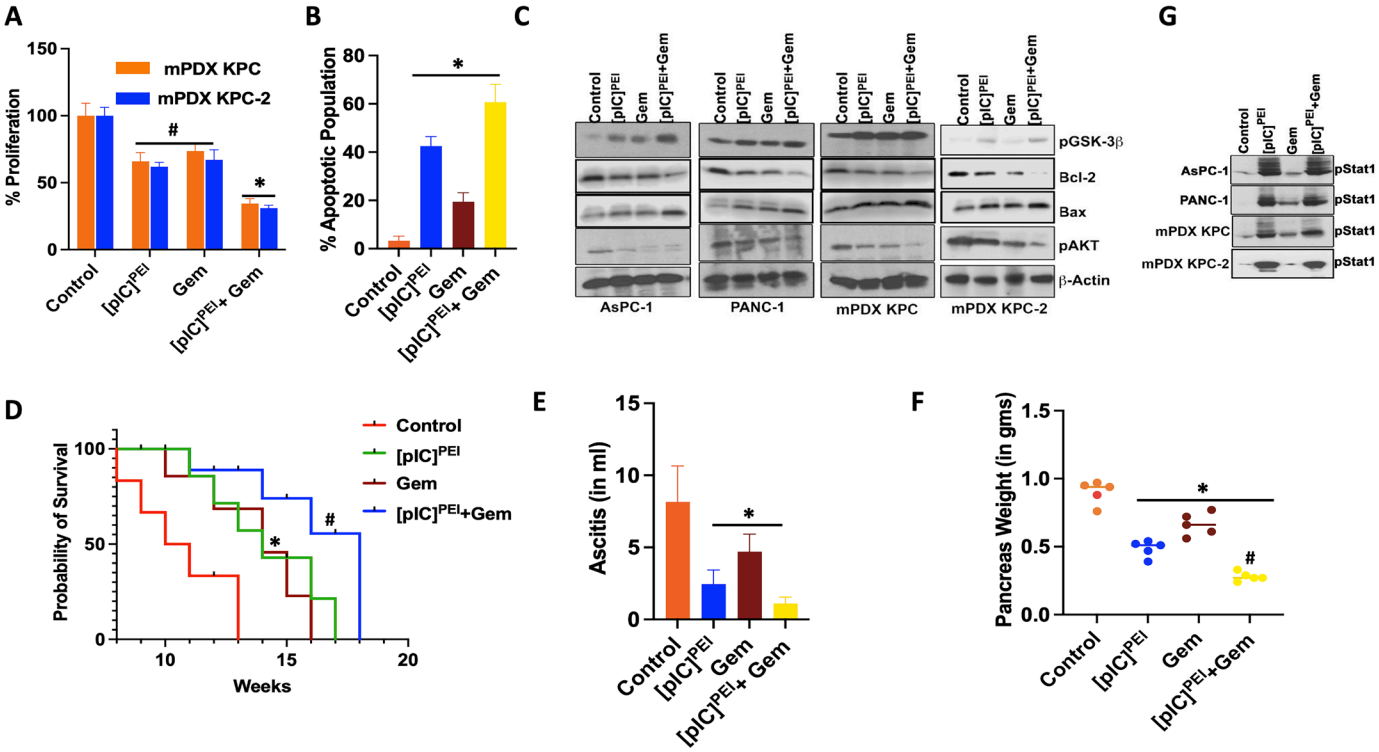

Figure 7 [pIC]^{PEI} enhances gemcitabine sensitivity in PDAC. (A) mPDX KPC or mPDX KPC-2 cells were plated in 96-well plates and treated with either gemcitabine (Gem) alone, or [pIC]^{PEI} (0.5 µg/mL) alone, or in combination for 48 hours and MTT assays were performed. Data presented as % proliferation. (B) mPDX KPC cells were treated as described in A. Annexin V staining was performed, and data presented as % apoptotic cells. (C) Human or mouse PDAC cells were treated as described in A. Western blotting analysis was performed for different pro-apoptotic and anti-apoptotic markers. (D) Kaplan-Meier survival curves showing enhanced survival in homozygous p53 KPC mice treated with [pIC]^{PEI} (1 mg/kg dose, eight injections) or Gem (10 mg/kg, 8 injections) alone or in combination. Average ascites volume (E) and average (and individual) pancreas weights (F) from KPC mice from D. (G) Western blotting analysis for pStat1 in the indicated cells treated with either Gem (5 µM) or [pIC]^{PEI} (0.5 µg/mL) alone, or in combination for 48 hours. *, p<0.01 compared with control, #, p<0.05 compared with control. MTT, 3-(4,5-dimethylthiazol-2-yl)–2,5-diphenyltetrazolium bromide; PDAC, pancreatic ductal adenocarcinoma; PEI, polyethyleneimine; pIC, polyinosine–polycytidylic acid.

investigations are required to elucidate the additional potential molecular mechanism(s) involved when PDAC are treated with [pIC]^{PEI} plus Gem. In conclusion, our findings demonstrate enhanced therapeutic effects in PDAC when [pIC]^{PEI} and a SOC treatment chemotherapy, Gem, are used in combination.

DISCUSSION

Pancreatic cancer remains a formidable foe and one of the most difficult cancers to treat effectively.[36] Rapid disease progression and late diagnosis after a primary tumor has metastasized contribute to treatment failures.[37] Moreover, the lack of efficacy of current treatment modalities emphasizes the need for new approaches to combat this lethal neoplasm. Delivering pIC into the cytosol with PEI, [pIC]^{PEI}, selectively promotes PDAC apoptosis without negatively affecting normal pancreatic epithelial cells or animal health.[11] Antitumor effects are evident both in cultured human cells and in vivo in human PDAC xenograft nude mouse models, subcutaneous tumor injection and quasi-orthotopic intraperitoneal delivery.[11] Using transgenic animal models of PDAC, with an intact immune system, we now elucidate the mechanism of [pIC]^{PEI} cancer selectivity, which involves macrophage polarization mediated in part by Stat1 activation, followed by CCL2 and MMP13 activation. Considering its safety profile, ability to synergize with SOC therapeutics, such as Gem, potent immune activating capacity and absence of toxicity toward normal cells,[11] [pIC]^{PEI} may provide a viable future therapy for PDAC.

The [pIC]^{PEI} potently suppresses tumor growth and metastasis in human melanoma, breast cancer, hepatoma and PDAC (in nude mice).[12–14] We now demonstrate that intraperitoneal administration of [pIC]^{PEI} in heterozygous or homozygous KPC transgenic mice significantly decreases tumor volume and tumor mass and increases survival relative to control KPC animals. The presence of ascites in patients with PDAC is a predictor of active disease progression, connoting poor prognosis.[38] [pIC]^{PEI} treatment inhibited both tumor growth and reduced ascites fluid volume, contributing to a decrease in abdominal pressure and distension, enhancing survival. Pretreatment of KPC mice with [pIC]^{PEI} also induced a vaccine (memory) effect that was associated with induction of

increased IFN-γ, and CD8 expression in tumors as well as in splenocytes (figure 2). These studies emphasize robust anti-PDAC short-term (direct apoptotic/immune-mediated elimination) and long-term (vaccine prevention) activity of [pIC]^{PEI} in the context of animals with intact immune systems.

Increased levels of IL-6 on [pIC]^{PEI} treatment may signal increased immune-mediated cancer cell death in these KPC animals. IL-6 trans-signaling has numerous effects on immune cells and the vasculature that cooperate to orchestrate effective antitumor immunity. IL-6 is essential for promoting T-cell trafficking to tumor sites and lymph nodes, where they can activate and perform their cytotoxic effector roles, respectively.[39]

Tumor-reactive T cells are primary contributors in cancer immunotherapy.[40] Stimulating T-cell responses promotes elimination or reduction in established tumor growth and metastasis.[41 42] Lack of effector T-cell trafficking and penetration into the tumor parenchyma are major obstacles to all T cell-based cancer immunotherapies.[23] In this context, the observation that systemic administration of [pIC]^{PEI} increases CD8+ T-cell infiltration into the tumor parenchyma and reduces PDAC development in mice make it a viable option to enhance T cell-based immunotherapeutic responses. These aspects of [pIC]^{PEI} action are areas worthy of future investigation.

Since IFN-γ promotes systemic cytokine release following [pIC]^{PEI} treatment, we considered a functional role of IFN-γ in stimulating tumor-infiltrating monocytes displaying anti-fibrotic activity. CCL2 is required for anti-CD40 therapy to recruit anti-fibrotic monocytes to PDAC tumors.[22] CCL2 produced by both malignant and non-malignant cells recruits monocytes to metastatic breast cancer lesions.[43] The IFN-γ/Stat1 axis regulates CCL2,[44] which correlates with our results indicating that [pIC]^{PEI} increases CCL2 levels in a Stat1-dependent manner in KPC mouse tumors (figure 4). MMP13 expressed in inflammatory monocytes can degrade both collagen and fibrin (FN), important components in the antifibrotic process and CCL2 is capable of regulating MMP13 activity (online supplemental figure S11). The [pIC]^{PEI} treatment of KPC mice elevates levels of MMP13 in tumors and decreases fibrosis (online supplemental figure S16, S17). These results indicate that [pIC]^{PEI} treatment of KPC mice increases Stat1 activation resulting in a CCL2-mediated increase in MMP13.

Stat1 is critical in both the innate and adaptive arms of immunity[45] and expression promotes an IFN-dependent immune response against chemically-induced tumors in immunocompetent mice.[46] M1 macrophages, commonly known as inflammatory macrophages increase when the IFN-γ/Stat1 pathway is activated, resulting in tumor death through production of reactive oxygen/nitrogen species.[47] [pIC]^{PEI} increases M1 macrophages and decreases M2 macrophages in KPC mice and blocking CCL2 inhibits this M1 polarization resulting in inhibition of [pIC]^{PEI}-mediated tumor regression. Blocking CCL2 decreases MMP13 levels without altering Stat1 levels suggesting that CCL2 functions upstream of MMP13 and downstream of Stat1. Inhibiting MMP13 with an MMP13-specific inhibitor (MMP13-I) blocks MMP13 expression and decreases M1 polarization without changing CCL2 or Stat1 levels (figure 6). These studies confirm that MMP13 works downstream of both of these molecules to regulate M1 polarization. Support for this conclusion, that is, CCL2 and MMP13 induction by [pIC]^{PEI} enhance M1 and decrease M2 polarization, was provided using specific inhibitors in BMDM. Taken together these results demonstrate that [pIC]^{PEI} activates immune-mediated tumor regression via the IFN-γ-Stat1-CCL2-MMP13 axis by increasing M1 macrophages in tumors as well as in the spleen. Immunofluorescence data from tumor sections from [pIC]^{PEI} treated animals indicated an increase in T-cell and macrophage accumulation (online supplemental figure S17) with elevated levels of Stat1 and MMP-13 expression in [pIC]^{PEI} treated animal tissue.

The [pIC]^{PEI} antitumor activity, both in vitro in established human and mouse PDAC cells and in vivo in KPC immunocompetent mice, is enhanced further when combined with Gem, a SOC drug in PDAC (figure 7D, online supplemental figure S14). Combining [pIC]^{PEI} with Gem did not increase Stat1 phosphorylation further implicating additional pathway(s) in enhancing therapeutic activity. A recent study demonstrates that HSP90 and its co-chaperone SUGT1 directly maintain the stability of STAT1 protein and subsequent transcriptional activation of immune checkpoint expression downstream of IFN signaling.[48] Although [pIC]^{PEI} increased expression of programmed cell death protein 1 (PD-1) and programmed cell death ligand 1 (PD-L1) (online supplemental figure S18), further experiments are needed to decipher whether [pIC]^{PEI}-mediated activation of Stat1 can regulate checkpoint protein expression in these animals.

In summary, [pIC]^{PEI} causes AKT-XIAP-mediated apoptosis in vitro and in vivo in human and murine PDAC and promotes IFNγ-Stat1-CCL2-mediated macrophage differentiation leading to T-cell activation in immune competent mice, ultimately reducing tumor/ascites burden and enhancing survival. Additionally, the therapeutic activity of [pIC]^{PEI} in PDAC is enhanced with Gem, significantly expanding therapeutic possibilities. One possible mechanism behind this combinatorial beneficial effect could be increased ENT1 expression observed in [pIC]^{PEI} treated animal tumor tissues, which is a Gem transporter (online supplemental figure S19). A phase I clinical trial (NCT02828098) recently evaluated BO-112 ([pIC]^{PEI}) in patients with aggressive solid tumors following a single intratumoral (IT) injection (Part 1; N=16) and after a combination of IT BO-112 ([pIC]^{PEI}) with pembrolizumab or nivolumab (Part 2; N=28)[49] (NCT04570332). In the Part 2 combination trial an ORR of 11% and DCR of 46% was observed in patients with multiple tumor types, not including PDAC. The safety profile of BO-112 ([pIC]^{PEI}), both as a single agent and in combination with anti-PD-1, was manageable. A phase 2 clinical study of IT BO-112 ([pIC]^{PEI}) in combination with

pembrolizumab is currently ongoing.[49 50] Since both safety profiles of [pIC]^{PEI} and Gem are now established, the relevance of our current studies carries even more weight. Considering the current preclinical data in the context of immune competent KPC mice, further evaluation is merited for the rapid translation into the clinic of [pIC]^{PEI} to treat patients with PDAC to determine efficacy against this invariably fatal cancer.

Author affiliations
[1]Human and Molecular Genetics, Virginia Commonwealth University, School of Medicine, Richmond, Virginia, USA
[2]VCU Institute of Molecular Medicine, Virginia Commonwealth University, School of Medicine, Richmond, Virginia, USA
[3]VCU Massey Comprehensive Cancer Center, Virginia Commonwealth University, School of Medicine, Richmond, Virginia, USA
[4]Surgery, Division of Surgical Oncology, Virginia Commonwealth University, School of Medicine, Richmond, Virginia, USA
[5]Biochemistry and Molecular Biology, Virginia Commonwealth University, School of Medicine, Richmond, Virginia, USA

Correction notice This article has been corrected since it was first published online. An incorrect set of Western blots were used for XIAP and beta-actin samples in mPDX KPC (Fig 1B left panel) when preparing Fig. 1B. The original Western blots were located, and a corrected Fig. 1B is now provided.

Acknowledgements The present study was supported in part by the Thelma Newmeyer Corman Endowment (PF), developmental funds from the VCU Institute of Molecular Medicine (PB, LE, SKD, PF), research support from the Department of Human and Molecular Genetics (PB, LE) and National Cancer Institute Cancer Center Support Grant to VCU Massey Cancer Center P30 CA16059. We thank Yee Aung and Daniel Sanchez De La Rosa for excellent technical assistance.

Contributors Conception and design: PB, LE, PBF. Development of methodology: PB, AK, AKP, SM, PM, JJW, MAS, DZ, VV. Acquisition of data: PB, AK, AKP, SM, PM, JJW, MAS, DZ, VV, EM. Analysis and interpretation of data: PB, JGT, AA, DS, RG, SKD, LE, PBF. Writing, review, and/or revision of the manuscript: PB, LE, PBF. Study supervision: LE, SKD, PBF. PB, LE and PBF are responsible for overall content as the guarantors.

Funding The present study was supported in part by the National Foundation for Cancer Research (NFCR) (PBF), Thelma Newmeyer Corman Endowment (PBF), Human and Molecular Genetics Development Fund (SKD, LE, PB, AKP), VCU Institute of Molecular Medicine (VIMM) (AK, SM, PM), Massey Pilot Research Grant (LE, PBF), and NIH-NCI Cancer Center Support Grant P30 CA016059 (JJW, DZ, VV, JGT, EM, DS, RG, SKD, LE, PBF).

Competing interests None declared.

Patient consent for publication Not applicable.

Ethics approval Not applicable.

Provenance and peer review Not commissioned; externally peer reviewed.

Data availability statement All data relevant to the study are included in the article or uploaded as supplementary information.

ORCID iD
Paul B Fisher http://orcid.org/0000-0002-0085-4546

REFERENCES

1 Orth M, Metzger P, Gerum S, *et al*. Pancreatic Ductal adenocarcinoma: biological hallmarks, current status, and future perspectives of combined modality treatment approaches. *Radiat Oncol* 2019;14:141.
2 Rahib L, Smith BD, Aizenberg R, *et al*. Projecting cancer incidence and deaths to 2030: the unexpected burden of thyroid, liver, and Pancreas cancers in the United States. *Cancer Res* 2014;74:2913–21.
3 Siegel RL, Miller KD, Fuchs HE, *et al*. Cancer statistics, 2022. *CA Cancer J Clin* 2022;72:7–33.
4 Adamska A, Domenichini A, Falasca M. Pancreatic Ductal adenocarcinoma: current and evolving therapies. *Int J Mol Sci* 2017;18:1338.
5 Narayanan S, Vicent S, Ponz-Sarvisé M. PDAC as an immune evasive disease: can 3d model systems aid to tackle this clinical problem? *Front Cell Dev Biol* 2021;9:787249.
6 Wörmann SM, Diakopoulos KN, Lesina M, *et al*. The immune network in Pancreatic cancer development and progression. *Oncogene* 2014;33:2956–67.
7 Caskey M, Lefebvre F, Filali-Mouhim A, *et al*. Synthetic double-stranded RNA induces innate immune responses similar to a live viral vaccine in humans. *J Exp Med* 2011;208:2357–66.
8 Zainol MIB, Kawasaki T, Monwan W, *et al*. Innate immune responses through toll-like receptor 3 require human-antigen-R-mediated Atp6V0D2 mRNA stabilization. *Sci Rep* 2019;9:20406.
9 Wu J, Huang S, Zhao X, *et al*. Poly(I:C) treatment leads to interferon-dependent clearance of hepatitis B virus in a Hydrodynamic injection mouse model. *J Virol* 2014;88:10421–31.
10 De Waele J, Verhezen T, van der Heijden S, *et al*. A systematic review on Poly(I:C) and poly-ICLC in glioblastoma: Adjuvants coordinating the unlocking of Immunotherapy. *J Exp Clin Cancer Res* 2021;40:213.
11 Bhoopathi P, Quinn BA, Gui Q, *et al*. Pancreatic cancer-specific cell death induced in vivo by cytoplasmic-delivered Polyinosine-Polycytidylic acid. *Cancer Res* 2014;74:6224–35.
12 Tormo D, Checińska A, Alonso-Curbelo D, *et al*. Targeted activation of innate immunity for therapeutic induction of Autophagy and apoptosis in Melanoma cells. *Cancer Cell* 2009;16:103–14.
13 Besch R, Poeck H, Hohenauer T, *et al*. Proapoptotic signaling induced by RIG-I and MDA-5 results in type I interferon-independent apoptosis in human Melanoma cells. *J Clin Invest* 2009;119:2399–411.
14 Mehrotra S, Britten CD, Chin S, *et al*. Vaccination with Poly(IC:LC) and peptide-pulsed Autologous Dendritic cells in patients with Pancreatic cancer. *J Hematol Oncol* 2017;10:82.
15 Martins KAO, Bavari S, Salazar AM. Vaccine adjuvant uses of poly-IC and derivatives. *Expert Rev Vaccines* 2015;14:447–59.
16 Peng SF, Hsu HK, Lin CC, *et al*. Novel PEI/poly-gamma-Gutamic acid nanoparticles for high efficient siRNA and Plasmid DNA Co-delivery. *Molecules* 2017;22:86.
17 Domankevich V, Efrati M, Schmidt M, *et al*. n.d. RIG-1-like receptor activation Synergizes with Intratumoral alpha radiation to induce Pancreatic tumor rejection, triple-negative breast metastases clearance. *Front Oncol*;10.
18 Inao T, Harashima N, Monma H, *et al*. Antitumor effects of cytoplasmic delivery of an innate adjuvant receptor ligand. *Breast Cancer Res Treat* 2012;134:89–100.
19 Peng S, Geng J, Sun R, *et al*. Polyinosinic-Polycytidylic acid Liposome induces human hepatoma cells apoptosis which correlates to the up-regulation of RIG-I like receptors. *Cancer Sci* 2009;100:529–36.
20 Yip-Schneider MT, Wu H, Hruban RH, *et al*. Efficacy of Dimethylaminoparthenolide and sulindac in combination with Gemcitabine in a genetically engineered mouse model of Pancreatic cancer. *Pancreas* 2013;42:160–7.
21 Quinn BA, Dash R, Sarkar S, *et al*. Pancreatic cancer combination therapy using a Bh3 mimetic and a synthetic Tetracycline. *Cancer Research* 2015;75:2305–15.
22 Long KB, Gladney WL, Tooker GM, *et al*. Ifngamma and Ccl2 cooperate to redirect tumor-infiltrating monocytes to degrade fibrosis and enhance chemotherapy efficacy in Pancreatic carcinoma. *Cancer Discovery* 2016;6:400–13.
23 Anderson KG, Stromnes IM, Greenberg PD. Obstacles posed by the tumor Microenvironment to T cell activity: A case for synergistic therapies. *Cancer Cell* 2017;31:311–25.

24 Rao CV, Mohammed A, Janakiram NB, *et al*. Inhibition of Pancreatic intraepithelial Neoplasia progression to carcinoma by nitric oxide-releasing aspirin in P48(Cre/+)-LSL-Kras(G12D/+) mice. *Neoplasia* 2012;14:778–87.
25 Qing Y, Stark GR. Alternative activation of Stat1 and Stat3 in response to interferon-gamma. *J Biol Chem* 2004;279:41679–85.
26 Quigley M, Huang X, Yang Y. Stat1 signaling in Cd8 T cells is required for their Clonal expansion and memory formation following viral infection in vivo. *J Immunol* 2008;180:2158–64.
27 Richards DM, Hettinger J, Feuerer M. Monocytes and Macrophages in cancer: development and functions. *Cancer Microenviron* 2013;6:179–91.
28 Augier S, Ciucci T, Luci C, *et al*. Inflammatory blood monocytes contribute to tumor development and represent a privileged target to improve host Immunosurveillance. *J Immunol* 2010;185:7165–73.
29 Schmid MC, Varner JA. Myeloid cells in the tumor Microenvironment: modulation of tumor angiogenesis and tumor inflammation. *J Oncol* 2010;2010:201026.
30 Liang T, Chen J, Xu G, *et al*. Stat1 and Cxcl10 involve in M1 macrophage polarization that may affect Osteolysis and bone remodeling in Extrapulmonary tuberculosis. *Gene* 2022;809.
31 Koh YC, Yang G, Lai CS, *et al*. Chemopreventive effects of Phytochemicals and medicines on M1/M2 polarized macrophage role in inflammation-related diseases. *Int J Mol Sci* 2018;19:2208.
32 Slapak EJ, Duitman J, Tekin C, *et al*. Matrix Metalloproteases in Pancreatic Ductal adenocarcinoma. *Biology (Basel)* 2020;9.
33 Amrutkar M, Gladhaug IP. n.d. Pancreatic cancer Chemoresistance to Gemcitabine. *Cancers*;9:157.
34 Swayden M, Iovanna J, Soubeyran P. Pancreatic cancer Chemo-resistance is driven by tumor phenotype rather than tumor genotype. *Heliyon* 2018;4:e01055.
35 Kagawa S, Takano S, Yoshitomi H, *et al*. Akt/mTOR signaling pathway is crucial for Gemcitabine resistance induced by Annexin II in Pancreatic cancer cells. *J Surg Res* 2012;178:758–67.
36 Lambert A, Schwarz L, Borbath I, *et al*. An update on treatment options for Pancreatic adenocarcinoma. *Ther Adv Med Oncol* 2019;11:1758835919875568.
37 Kenner BJ, Chari ST, Maitra A, *et al*. Early detection of Pancreatic cancer-a defined future using lessons from other cancers: A white paper. *Pancreas* 2016;45:1073–9.
38 Baretti M, Pulluri B, Tsai H-L, *et al*. The significance of Ascites in patients with Pancreatic Ductal adenocarcinoma: A case-control study. *Pancreas* 2019;48:585–9.
39 Chen Q, Fisher DT, Clancy KA, *et al*. Fever-range thermal stress promotes lymphocyte trafficking across high endothelial Venules via an interleukin 6 Trans-signaling mechanism. *Nat Immunol* 2006;7:1299–308.
40 Gonzalez H, Hagerling C, Werb Z. Roles of the immune system in cancer: from tumor initiation to metastatic progression. *Genes Dev* 2018;32:1267–84.
41 Ott PA, Wu CJ. Cancer vaccines: steering T cells down the right path to eradicate tumors. *Cancer Discov* 2019;9:476–81.
42 Waldman AD, Fritz JM, Lenardo MJ. A guide to cancer Immunotherapy: from T cell basic science to clinical practice. *Nat Rev Immunol* 2020;20:651–68.
43 Qian B-Z, Li J, Zhang H, *et al*. Ccl2 recruits inflammatory monocytes to facilitate breast-tumour metastasis. *Nature* 2011;475:222–5.
44 Moore F, Naamane N, Colli ML, *et al*. Stat1 is a master regulator of Pancreatic {Beta}-Cell apoptosis and islet inflammation. *J Biol Chem* 2011;286:929–41.
45 Jung SR, Ashhurst TM, West PK, *et al*. Contribution of Stat1 to innate and adaptive immunity during type I interferon-mediated lethal virus infection. *PLoS Pathog* 2020;16:e1008525.
46 Kaplan DH, Shankaran V, Dighe AS, *et al*. Demonstration of an interferon gamma-dependent tumor surveillance system in immunocompetent mice. *Proc Natl Acad Sci U S A* 1998;95:7556–61.
47 Arora S, Dev K, Agarwal B, *et al*. Macrophages: their role, activation and polarization in pulmonary diseases. *Immunobiology* 2018;223:383–96.
48 Liu K, Huang J, Liu J, *et al*. n.d. Hsp90 mediates Ifngamma-induced adaptive resistance to anti-PD-1 Immunotherapy.
49 Alvarez M, Molina C, De Andrea CE, *et al*. Intratumoral Co-injection of the poly I:C-derivative BO-112 and a STING agonist Synergize to achieve local and distant anti-tumor efficacy. *J Immunother Cancer* 2021;9:e002953.
50 Márquez-Rodas I, Longo F, Rodriguez-Ruiz ME, *et al*. Intratumoral Nanoplexed poly I:C BO-112 in combination with systemic anti-PD-1 for patients with anti-PD-1-refractory tumors. *Sci Transl Med* 2020;12:eabb0391.